

Longitudinal assessment of fractional anisotropy alterations caused by simian immunodeficiency virus infection: a preliminary diffusion tensor imaging study

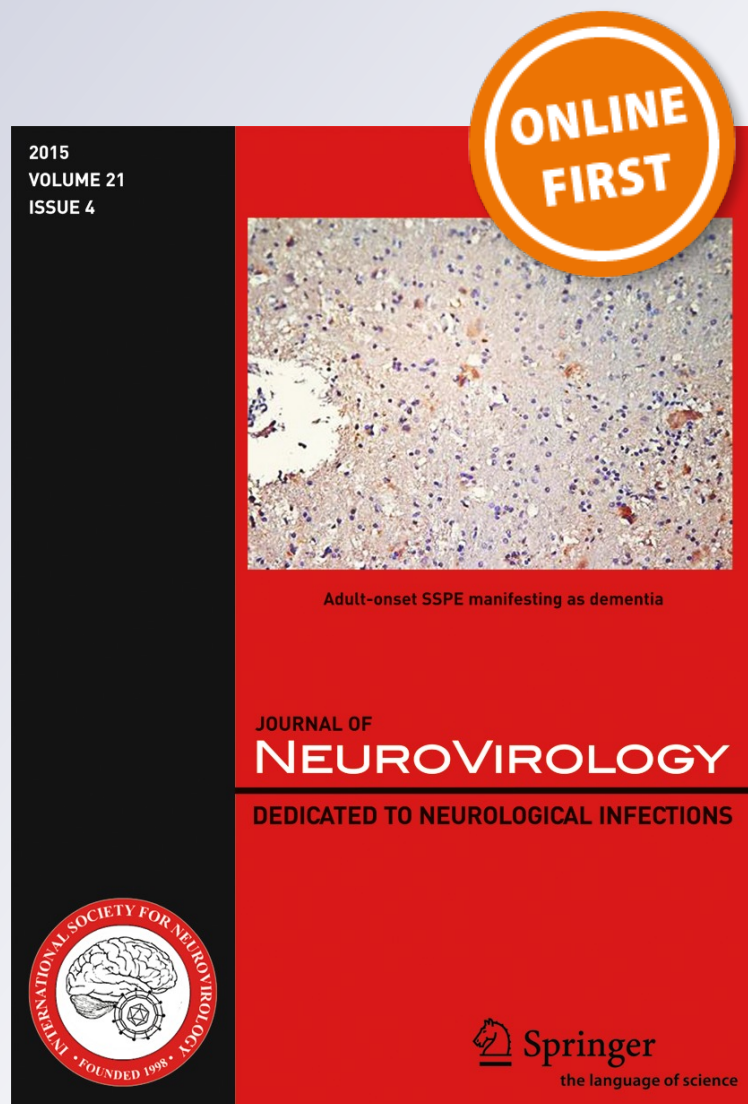
Zhenchao Tang, Enqing Dong, Jiaojiao Liu, Zhenyu Liu, Wenjuan Wei, Bo Wang, Hongjun Li & Jie Tian

Journal of NeuroVirology

ISSN 1355-0284

J. Neurovirol.

DOI 10.1007/s13365-015-0388-1



Your article is protected by copyright and all rights are held exclusively by Journal of NeuroVirology, Inc.. This e-offprint is for personal use only and shall not be self-archived in electronic repositories. If you wish to self-archive your article, please use the accepted manuscript version for posting on your own website. You may further deposit the accepted manuscript version in any repository, provided it is only made publicly available 12 months after official publication or later and provided acknowledgement is given to the original source of publication and a link is inserted to the published article on Springer's website. The link must be accompanied by the following text: "The final publication is available at link.springer.com".

Longitudinal assessment of fractional anisotropy alterations caused by simian immunodeficiency virus infection: a preliminary diffusion tensor imaging study

Zhenchao Tang¹ · Enqing Dong¹ · Jiaojiao Liu² · Zhenyu Liu³ · Wenjuan Wei³ · Bo Wang⁴ · Hongjun Li² · Jie Tian³

Received: 10 April 2015 / Revised: 8 September 2015 / Accepted: 21 September 2015
© Journal of NeuroVirology, Inc. 2015

Abstract Previous diffusion tensor imaging (DTI) studies found that human immunodeficiency virus (HIV) infection led to white matter (WM) microstructure degeneration. Most of the DTI studies were cross-sectional and thus merely investigated only one specific point in the disease. In order to systematically study the WM impairments caused by HIV infection, more longitudinal studies are needed. However, longitudinal studies on HIV patients are very difficult to conduct. To address this question, we employed the simian immunodeficiency virus (SIV)-infected rhesus monkeys model to carry out a longitudinal DTI study. We aimed to longitudinally assess the WM abnormalities of SIV-infected rhesus monkeys by studying the fractional anisotropy (FA) alterations with

Tract Based Spatial Statistic (TBSS) analysis. Four rhesus monkeys inoculated intravenously with SIVmac239 were utilized in the study. DTI scans and peripheral blood CD4⁺ and CD8⁺ T cell counts were acquired prior to virus inoculation (as the baseline) and in the 12th and 24th week postvirus inoculation. Significant FA alterations were found in the two areas of the inferotemporal regions (iTE), respectively located in the ventral subregion of posterior iTE (iTEpv) and the dorsal subregion of iTE (iTEpd). The decreased FA values in iTEpd were found significantly negatively correlated with the elevated peripheral blood CD4⁺/CD8⁺ ratios. It might suggest that WM in iTEpd was still impaired even though the immune dysfunction alleviated temporally.

Zhenchao Tang, Enqing Dong and Jiaojiao Liu contributed equally to this work.

Electronic supplementary material The online version of this article (doi:10.1007/s13365-015-0388-1) contains supplementary material, which is available to authorized users.

✉ Enqing Dong
enqdong@sdu.edu.cn

✉ Hongjun Li
lihongjun00113@126.com

✉ Jie Tian
tian@ieee.org

¹ School of Mechanical, Electrical & Information Engineering, Shandong University, Weihai, Shandong Province 264209, China

² Beijing YouAn Hospital, Capital Medical University, Beijing 100069, China

³ Key Laboratory of Molecular Imaging, Institute of Automation, Chinese Academy of Sciences, Beijing 100190, China

⁴ School of Automation, Harbin University of Science and Technology, Harbin 150080, China

Keywords Simian immunodeficiency virus · Longitudinal study · Diffusion tensor imaging · Fractional anisotropy · Tract-based spatial statistic

Introduction

The introduction of highly active anti-retroviral therapy (HAART) and combination antiretroviral therapy (cART) greatly reduces the mortality of HIV-infected patients and prolongs their life expectancy. While the antiretroviral therapy remarkably improves survival of the HIV patients, most of the therapies are insufficient to remove the brain injury of the HIV infection (Ellis et al. 2007). Although the HIV associated dementia (HAD) is rarely seen among the HIV patients under potent antiretroviral therapy, the HIV associated neurocognitive disorder (HAND) still persists in the HAART era (Clifford and Ances 2013; Heaton et al. 2010). The neurobiological mechanism of HAD and HAND remains incompletely understood (Gongvatana et al. 2009). Previous pathological study suggested that

the white matter (WM) was preferentially injured in HIV patients (Bell 1998). A previous *in vivo* neuroimaging study found more extensive WM abnormalities in HAD than nondemented HIV patients, and the WM abnormalities were associated with the worsening cognitive impairment in HAD (Chen et al. 2009). Further studies of the WM abnormalities in HIV infection might potentially provide more insight into the underlying mechanisms of the cognitive decline that can be seen in HIV subjects in the HAART era.

DTI is an *in vivo* neuroimaging method sensitive to detect subtle WM abnormalities (Schouten et al. 2011). The technique is especially helpful in studying disease associated with demyelination and axonal damage, which are commonly seen in HIV infection (Anthony and Bell 2008; Medana and Esiri 2003). Previous DTI studies found significant WM injuries in HIV patients indicated by the abnormalities in fractional anisotropy (FA), mean diffusivity (MD), axial diffusivity (AD), and radial diffusivity (RD). Early DTI studies found WM damage in the prefrontal WM and corpus callosum by region-of-interests (ROI)-based analysis (Pfefferbaum et al. 2007; Wu et al. 2006). Subsequent studies employing whole brain voxel-based analysis found that more widespread WM regions were impaired by HIV infection, including the temporal and parietal WM (Chen et al. 2009). More recently, tract-based spatial statistics (TBSS) was utilized in the DTI study of HIV patients (Leite et al. 2013; Zhu et al. 2013). TBSS studies found that the temporal WM, parietal WM, corpus callosum, and corona radiata were involved in HIV infection (Zhu et al. 2013). DTI provided a non-invasive and convenient method to study the WM abnormalities of HIV-infected patients, and the findings were consistent with previous HIV neuropathology research studies (Anthony and Bell 2008). Previous neuropathology studies of HIV encephalitis found that the white matter of cerebral hemispheres and the corpus callosum were preferentially invaded by the macrophages and multinucleated giant cells, which indicated the progression of neuroinflammatory processes (Gosztanyi et al. 1994). Previous autopsy studies of HIV patients also found axonal damage and demyelination in the subcortical and deep white matter (Langford et al. 2002; Raja et al. 1997).

Most of previous DTI studies on HIV patients were cross-sectional (Masters and Ances 2014). Cross-sectional studies investigated the HIV cohorts on a specific point of time, and they were efficient to detect the WM abnormalities in HIV infection (Chen et al. 2009; Correa et al. 2015). However, the cross-sectional studies were limited because they only generated a single snapshot of disease point, and they were unable to follow the WM abnormalities from early to late stages of the disease. Longitudinal studies are needed to provide information about whether the WM abnormalities in HIV

infection are permanent, static, or progressive (Gongvatana et al. 2011; Hoare et al. 2012).

Conducting longitudinal studies on human subject can be challenging for reasons such as difficulty determining the precise time of infection and patient noncompliance. To circumvent these difficulties, an appropriated animal model parallel to human infected with HIV can be used. Rhesus monkeys infected with simian immunodeficiency virus (SIV) resemble HIV patients strongly in neuropathological manifestations, providing an ideal model for studying WM abnormalities in AIDS infection (Burudi and Fox 2001; Gold et al. 1998; Murray et al. 1992; Williams et al. 2008). In addition, previous neuroimaging study also found that SIV-infected rhesus monkeys exhibited DTI indices abnormalities similar to HIV patients (Li et al. 2011). Thus, conducting longitudinal DTI study on SIV-infected rhesus monkeys would reproduce the whole pathogenesis of WM injuries in SIV infection and provide insight into the HIV-associated WM abnormalities.

In our study, we aimed to longitudinally study the WM abnormalities of the SIV-infected rhesus monkeys by TBSS analysis on FA values alterations. TBSS focused on large WM tracts in a voxel-wise manner, combining the strengths of ROI-based and whole brain voxel-based analysis (Smith et al. 2006). Peripheral blood indices, including CD4⁺ and CD8⁺ T cell counts, were also obtained to investigate the relationship of these clinical measures to the DTI findings.

Materials and methods

Subjects

Experiments were approved by Beijing Municipal Sciences & Technology Commission. Four male rhesus monkeys (ages 3–5 years) of Chinese origin were utilized in our longitudinal study. All the animals underwent health screening and were confirmed to be healthy before being assigned to the project. Indirect immunofluorescent assay (IFA) was also employed to exclude the potential infection of simian immunodeficiency (SIV), simian type-D retrovirus (SRV), or simian T cell lymphotropic virus-I (STLV-I). All of the four monkeys were inoculated intravenously with SIVmac239. MRI scans were acquired prior to virus inoculation (as the baseline) and in the 12th and 24th week postvirus inoculation. All the animals had laboratory evaluations (peripheral blood CD4⁺, CD8⁺ T cell counts, plasma SIV RNA viral load, and white cell counts) performed before each MRI scan. In the preparation for imaging and T cells counts, the animals were anesthetized by intramuscular injection of ketamine hydrochloride (5–10 mg/kg). The body temperature of each animal was monitored during the MRI scan, and a water blanket was used to prevent hypothermia. The details of the body temperature and laboratory evaluation values are shown in Table A1 of the

supplement. The serial numbers of the animals were 130005, 130007, 130010, and 130011. Monkey 130007 died of terminal AIDS in the 13th week.

Animals were housed at the Institute of laboratory animal sciences, CAMs & PUMC (Chinese Academy of Medical Sciences & Peking Union Medical College). The housing surroundings were maintained at 16~26 °C, humidity 40~70 %, and 12-h/12-h light/dark cycle. Water was available ad libitum. Monkeys formula feeds were provided on a twice-daily regimen without dietary restrictions. All animals were housed according to the standards of Institute of laboratory animal sciences, CAMs & PUMC.

DTI scan protocol

The DTI scans were acquired three times on each animal for the longitudinal assessment of SIV infection. All DTI scans were performed using a 3T Siemens Tim TRIO whole-body magnetic resonance scanner (Siemens, Germany) with a 32-channel head coil at Beijing YouAn Hospital, Capital Medical University. For each animal, structural and diffusion weighted MRI scans were obtained after the animal was anesthetized and placed in the supination position. T1 weighted images were acquired with a turbo flash sequence. The parameters were repetition time/echo time (TR/TE)=1800/4.5 ms, FOV=160 mm×160 mm, data matrix=320×320, flip angle=9°, slice thickness=1 mm (voxel size=0.5×0.5×1.0 mm³). Scan time was 7 min 50 s. A turbo spin echo (TSE) sequence in the axial orientation was used in the DTI scans. Diffusion weighted images (DWI) were acquired along 30 noncollinear and noncoplanar directions with $b=800$ s/mm² and one $b=0$ s/mm² image. The parameters were TR/TE=4200/96 ms, FOV=160 mm×160 mm, data matrix=130×130, flip angle=90°, 28 slices with 2-mm slice thickness, and no gap (voxel size=1.2×1.2×2.0 mm³). The DTI scan was repeated four times and averaged to increase the signal-to-noise ratio. Scan time was 8 min 53 s.

T cell markers monitoring

Blood samples, for quantitation of peripheral blood CD4⁺ and CD8⁺ T cells, were collected before each DTI scan. CD4⁺/CD8⁺ ratios were then calculated from the peripheral blood CD4⁺ and CD8⁺ T cells counts.

DTI data analysis

Preprocessing

The FMRIB Software Library (FSL, FMRIB, Oxford, UK) (Smith 2002; Smith et al. 2004; Woolrich et al. 2009) was used in the data preprocessing. Firstly, all raw DWI volumes were aligned to the b0 image by EddyCorrect Tool to correct

for head motion and eddy current distortions. Then, the skull and nonbrain tissues were removed using Brain Extraction Tool (Smith 2002). Lastly, a diffusion tensor, or ellipsoid, was model at each voxel by Dtifit Tool (Basser et al. 1994). Based on the eigenvalues of the tensor, FA, MD, AD, and RD values were calculated on a voxel by voxel basis.

Tract-based spatial statistic

To identify all the major WM tracts in the brain, voxel-wise analysis on FA images was conducted using the TBSS toolbox of FSL (Smith et al. 2006). TBSS modified for processing nonhuman primate (NHP) brains was employed in our study, following the previous published approaches (Howell et al. 2014; Howell et al. 2013). Firstly, each FA image was nonlinearly registered to a common space or template. In our study, T1 template from Wisconsin 112RM-SL rhesus atlas (McLaren et al. 2009) was used as the target image. After registrations, all the images were in the coordinate space of Saleem-Logothetis rhesus brain stereotaxic atlas (Saleem and Logothetis 2012) and in the resolution of 0.5×0.5×0.5 mm³. Next, the registered images were averaged to create a mean FA image. The mean FA image was skeletonized by suppressing nonmax FA values perpendicular to the local tract structure, and then thresholded by 0.2 to create a mean FA skeleton. The threshold was used to exclude small peripheral tracts and suppress high inter-subject variability. After being thresholded, the mean FA skeleton represented the major WM tracts common to all the subjects. Lastly, all the registered FA images were projected onto the mean FA skeleton by filling the skeleton with FA values from the nearest relevant tract center. The skeletonized FA images were subsequently fed to statistical analysis. The raw TBSS maps were provided in the Fig. A1 of the supplement.

Statistical analysis

To uncover the WM impairments due to SIV infection, repeated measures ANOVA was performed on the skeletonized FA images from the three DTI scans. ANOVA analysis was conducted with the Randomise tool in FSL (Winkler et al. 2014). ANOVA results were thresholded at $P<0.005$ (uncorrected, cluster size ≥ 20). Anatomic regions which survived the threshold were then identified and labeled according to structures defined in Saleem-Logothetis rhesus brain stereotaxic atlas (Saleem and Logothetis 2012). Results were displayed in the T1 template from Wisconsin 112RM-SL rhesus atlas and considered as regions of interest (ROIs). The mean and max FA, AD, RD, and MD values were calculated in each ROI for each subject.

To access the longitudinal changes of the mean and max FA, AD, RD, and MD values in each ROI across all time points, three group comparisons were conducted with paired

t test analysis (baseline vs. 12th weeks, 12th weeks vs. 24th weeks and baseline vs. 24th weeks). Peripheral blood CD4⁺ T cell counts and CD4⁺/CD8⁺ ratios were analyzed in the same manner. Furthermore, we applied Pearson correlation between the diffusion parameters (the mean and max FA, AD, RD, and MD values) and peripheral blood indices (CD4⁺ T cell counts and CD4⁺/CD8⁺ ratios) to find out whether the WM impairments were related to the progression of HIV infection or immune dysfunction. The investigation was limited to the data acquired postvirus inoculation. Paired *t* test and Pearson correlation of SPSS 18 (<http://www-01.ibm.com/software/analytics/spss/>) were employed in the statistical analysis. Significance was set at $P < 0.05$.

The relationship of the diffusion parameters with the peripheral blood plasma SIV RNA viral load and the peripheral blood white cell counts was analyzed in the same manner. This issue was provided in the supplement.

Results

We found significant FA alterations in two areas of the inferotemporal regions (iTE) by repeated measure ANOVA. One was in the ventral subregion of posterior iTE (iTEpv, $P < 0.005$, uncorrected, 31 voxels, Fig. 1a), and the other was in the dorsal subregion of posterior iTE (iTEpd, $P < 0.005$, uncorrected, 20 voxels, Fig. 1b). Results were displayed in the T1 template from Wisconsin 112RM-SL rhesus atlas, which was in the coordinate space of Saleem-Logothetis rhesus brain stereotaxic atlas.

Longitudinal changes of the mean and max FA, AD, RD, and MD values in iTEpv and iTEpd are illustrated in Fig. 2. Comparing with baseline values, both the mean and max FA values in iTEpv significantly decreased in the 12th weeks postinoculation ($t = 4.353$, $P = 0.022$ for mean FA values; $t = 5.301$, $P = 0.013$ for max FA values). In comparison with the values of the 12th weeks, Max AD values in iTEpd

significantly decreased in the 24th weeks ($t = 5.743$, $P = 0.029$). No significant changes were observed in MD and RD values.

Longitudinal changes of peripheral blood CD4⁺ T cell counts and CD4⁺/CD8⁺ ratios are illustrated in Fig. 3. CD4⁺ T cell counts declined significantly in the 12th weeks in comparison with baseline values ($t = 5.77$, $P = 0.01$, Fig. 3a). CD4⁺/CD8⁺ ratios increased significantly in the 24th weeks in comparison with the values of 12th week ($t = -6.761$, $P = 0.021$, Fig. 3b).

For the data acquired postvirus inoculation, both the max and mean FA values in iTEpd were significantly negatively correlated with peripheral blood CD4⁺/CD8⁺ ratios ($r = -0.816$, $P = 0.025$ for mean FA; $r = -0.85$, $P = 0.015$ for max FA, scatter diagrams were showed in Fig. 4). The longitudinal analysis above revealed that the peripheral blood CD4⁺/CD8⁺ ratios significantly increased, while the max and mean FA values in iTEpd decreased nonsignificantly with the advance of disease. So, the decreased FA values in iTEpd were associated with the elevated peripheral blood CD4⁺/CD8⁺ ratios. No significant correlation was found between other diffusion parameters and peripheral blood indices.

The peripheral blood plasma SIV RNA viral load and the peripheral blood white cell counts showed no significant association with the diffusion parameters, and the details of the results are provided in the Table A2 and Table A3 of the supplement.

Discussion

In the current study, we longitudinally studied the FA alterations to access the WM impairments of the SIV-infected rhesus monkeys. Repeated DTI scans and peripheral blood indices were acquired at the baseline (2 weeks prior to virus inoculation) and in the 12th and 24th week postvirus inoculation. We found WM abnormalities in the inferotemporal

Fig. 1 3 × 1 repeated measures ANOVA results showed the main effect of time postinoculation. **a** Ventral subregion of posterior iTE (iTEpv, uncorrected, $P < 0.005$, 31 voxels). **b** Dorsal subregion of posterior iTE (iTEpd, uncorrected, $P < 0.005$, 20 voxels)

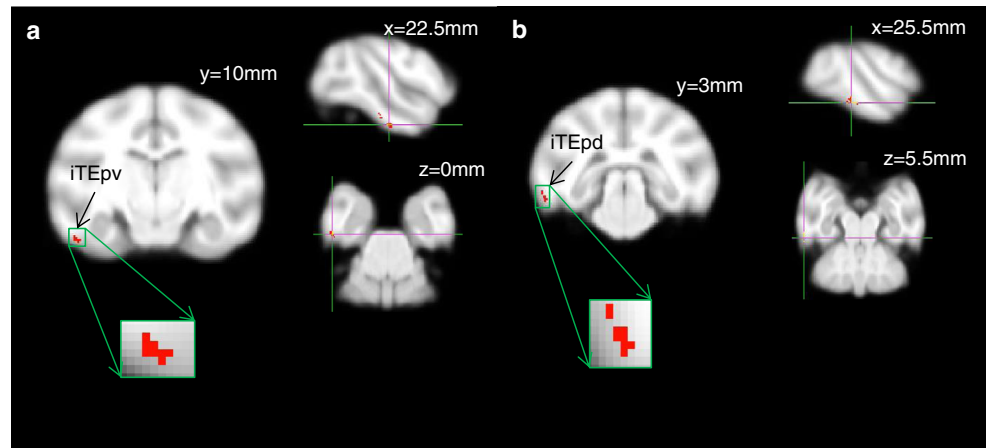
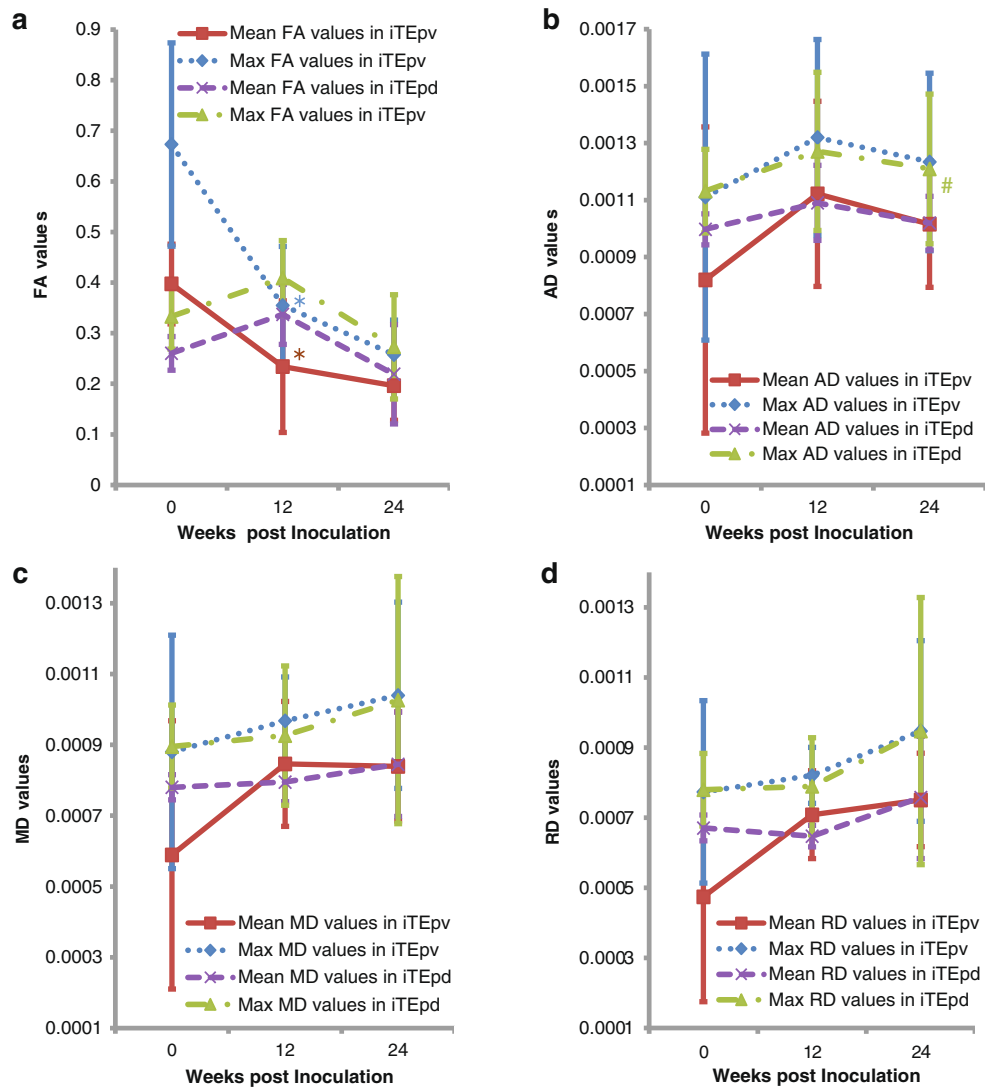


Fig. 2 Longitudinal changes of diffusion parameters in iTEpv and iTEpd after SIV inoculation. **a** Longitudinal changes of FA values in iTEpv and iTEpd. In comparison with baseline values, both the mean and max FA values in iTEpv significantly decreased in the 12th weeks postinoculation ($P=0.022$ for mean FA values; $P=0.013$ for max FA values). **b** Longitudinal changes of AD values in iTEpv and iTEpd. In comparison with the values of the 12th weeks postinoculation, max AD values in iTEpd significantly decreased in the 24th weeks postinoculation ($P=0.029$). **c** Longitudinal changes of MD values in iTEpv and iTEpd. No significant changes were found. **d** Longitudinal changes of RD values in iTEpv and iTEpd. No significant changes were found. Error bars represent standard deviation error. *, # $P<0.05$ compared with baseline and the 12th weeks, respectively



regions, and the WM abnormalities were associated with peripheral blood CD4⁺/CD8⁺ ratios.

The inferotemporal region of rhesus monkey corresponds anatomically to the inferior temporal region of human (Saleem and Logothetis 2012; Swards 2011a). Previous studies suggest that the homologies between the species also apply to white matter structures (Kravitz et al. 2011; Kravitz et al. 2013; Swards 2011b). Accumulating cross-sectional studies on HIV patients had reported neural lesions in the inferior temporal regions. In a previous DTI study examining the effect of clinical factors on the WM integrity of HIV patients, WM in the inferior temporal regions was found preferentially damaged due to hepatitis C virus (HCV) coinfection (Gongvatana et al. 2011). In addition to WM impairments, previous studies of HIV infection also found gray matter abnormalities in the inferior temporal regions (Becker et al. 2012; Kuper et al. 2011; Sarma et al. 2014). Kuper and his colleagues found severe gray matter atrophy in the left inferior temporal regions among HIV patients with cognitive

impairments (Kuper et al. 2011). Becker et al. not only identified HIV-related gray matter loss in the inferior temporal regions but also found significant correlation between the GM loss and performance of neuropsychological tests (Becker et al. 2012). Moreover, in an investigation on perinatally HIV-infected adolescents, gray matter hypertrophy was observed in bilateral inferior temporal regions, which might be the result of inflammation (Sarma et al. 2014). Our results of the SIV-associated WM impairments in the inferotemporal regions together with the findings of previous cross-sectional studies on HIV patients might suggest that the inferior temporal regions were vulnerable to both SIV and HIV infection.

The inferotemporal regions (iTE) are usually considered as the final stage in the ventral visual pathway and are crucial for visual objects recognition (Kravitz et al. 2011; Kravitz et al. 2013; Ohya et al. 2014). Our finding might suggest that SIV infection impaired the ventral visual pathway and may lead to disability or low efficiency of information transmission on the ventral visual pathway.

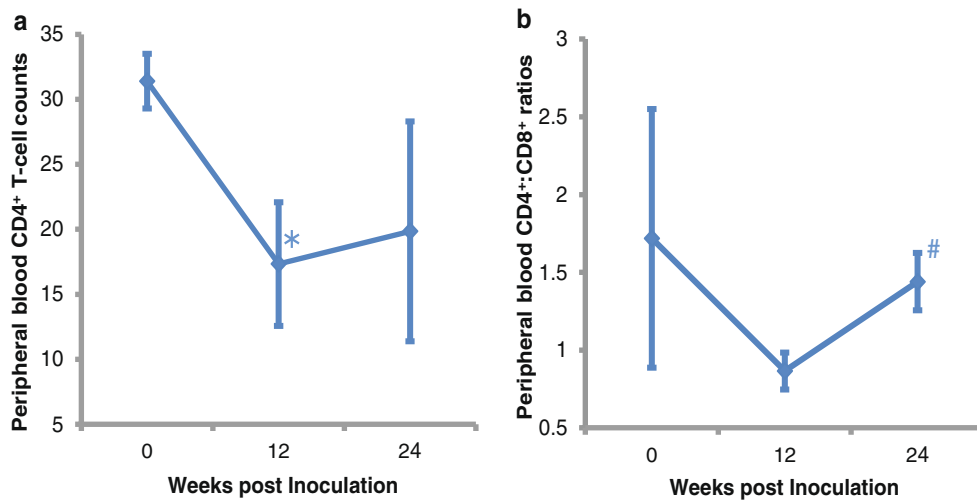


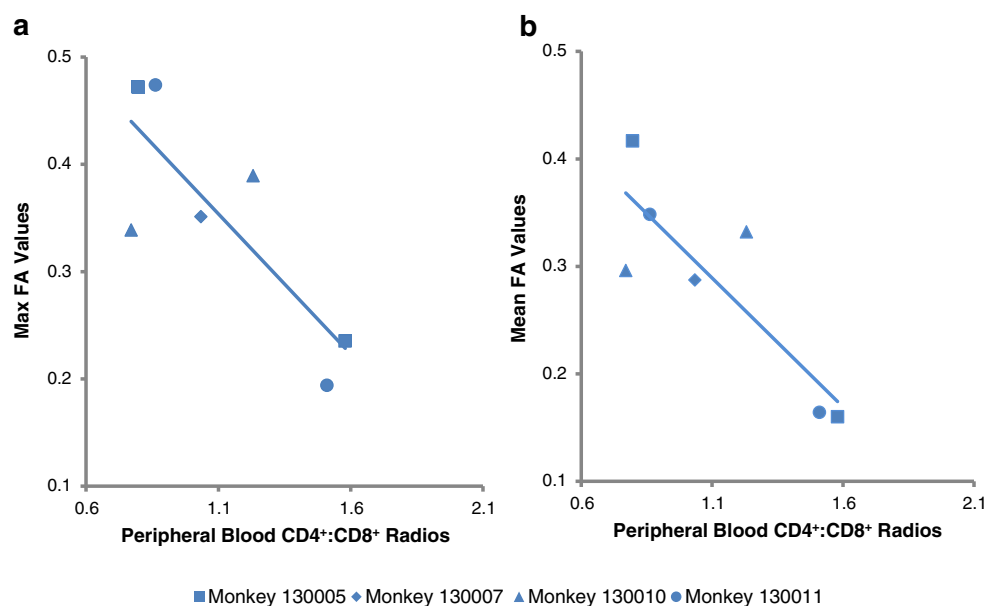
Fig. 3 Longitudinal changes of peripheral blood indices after SIV inoculation. **a** Longitudinal changes of peripheral blood CD4⁺ counts after SIV inoculation. In comparison with baseline values, CD4⁺ T cell counts declined significantly in the 12th week postinoculation ($P=0.01$). **b** Longitudinal changes of peripheral blood CD4⁺/CD8⁺ ratios after SIV

inoculation. In comparison with the values of the 12th week postinoculation, CD4⁺/CD8⁺ ratios increased significantly in the 24th week postinoculation ($P=0.021$). Error bars represent standard deviation error. *, # $P<0.05$ compared with baseline and the 12th weeks, respectively

In the longitudinal analysis, we found that both mean and max FA values in iTEpv significantly decreased in the 12th week compared with baseline values. FA decline was the most common finding of previous cross-sectional DTI studies on HIV patients (Correa et al. 2015; Gongvatana et al. 2009; Hoare et al. 2011; Stubbe-Drger et al. 2012). In the intact WM microstructure, water molecules diffusion perpendicular to the WM fibers was hindered by the myelin sheath, resulting distinct diffusivity anisotropy along the direction of the fiber and high FA values. Our results of decreased FA values in the iTEpv indicated that the diffusion pattern in the WM tissues was perturbed and WM microstructure of the iTEpv was damaged.

We found that the AD values in both iTEpd and iTEpv increased in the 12th week and decreased in the 24th week afterward. Specially, the max AD values in iTEpd significantly increased in the 24th week. Our finding of decreased AD values was consistent with one study of the HIV patients naive to combination antiretroviral therapy (cART) (Wright et al. 2012). However, several previous DTI studies also identified increased AD values in HIV patients (Leite et al. 2013; Nir et al. 2014; Zhu et al. 2013). The difference between our results and theirs might be due to the different pathological process of the WM degeneration that was identified. The increased AD values of HIV patients might be due to reduced axonal density or WM atrophy, which would increase the interstitial space between the

Fig. 4 Both the max and mean FA values in iTEpd were negatively correlated with peripheral blood CD4⁺/CD8⁺ ratios. **a** Max FA values in iTEpd were negatively correlated with CD4⁺/CD8⁺ ratios ($r=-0.816$, $P=0.025$, $R^2=0.665$). **b** Mean FA values in iTEpd were negatively correlated with CD4⁺/CD8⁺ ratios ($r=-0.85$, $P=0.015$, $R^2=0.723$)



axons and subsequently increase the water diffusion along the axonal direction (Zhu et al. 2013). Nevertheless, the decreased AD values caused by HIV infection might be associated with the severe injuries of highly aligned axonal fibers or the replacement of axonal fibers with less ordered cells such as glial cells, which could decrease the diffusivity along the axonal tracts (Sun et al. 2006; Wright et al. 2012). Our results might indicate that axonal injuries are the neuropathological process behind the SIV-associated WM abnormalities in iTEpd.

In our work, we found that the direction of AD values changed over time. Increased AD values were observed in the 12th week postinoculation, while decreased AD values were found in the 24th week postinoculation. It was noteworthy that the increased AD values were mostly reported among the HIV patients on a stable antiretroviral regimen, whose white matter damage was under control (Leite et al. 2013; Nir et al. 2014; Zhu et al. 2013). However, decreased AD values were observed in the HIV patients who were naive to antiretroviral therapy and had extensive WM damage (Wright et al. 2012). Our results might suggest that the WM was damaged further with advancing disease.

In HIV clinic, CD4⁺ T cell counts depletion is routinely used to evaluate disease progression and track disease development (Lentz et al. 2009). Our results of decreased CD4⁺ T cell indicated the developments of SIV infection. HIV infection would generally lead to CD4⁺ T cell counts depletion and CD8⁺ T cell counts augmentation, resulting the decrease of CD4⁺/CD8⁺ ratios. CD4⁺/CD8⁺ ratios decreasing were routinely associated with immune dysfunction, such as immunoactivation and immunosenescence (Sainz et al. 2013; Serrano-Villar et al. 2013), while we found increased CD4⁺/CD8⁺ ratios in the 24th week post-SIV inoculation and our results were consistent with previous SIV study which reported that the CD4⁺/CD8⁺ ratios would temporally recover after the initial decrease in the early stage of infection (Bao et al. 2014). In previous study, CD4⁺/CD8⁺ ratios elevation was also observed in HIV patients on antiretroviral treatment (ART) (Saracino et al. 2014; Serrano-Villar et al. 2013; Thornhill et al. 2014). Moreover, the increased CD4⁺/CD8⁺ ratios were found correlated with the accumulated ART exposure (Serrano-Villar et al. 2013). Our results might suggest that the immune dysfunction in SIV infection alleviated temporally to a certain extent by the 24th week postinoculation, though failed in reaching normal level. In addition, we also found that the increased CD4⁺/CD8⁺ ratios were negatively correlated with the decreased FA values in iTEpd. It might suggest that the WM in iTEpd was still impaired even though the immune dysfunction alleviated temporally.

The current study has several limitations. First, the sample size was small, and we could not adjust our analyses for multiple comparisons. Longitudinal studies with more animals investigated for longer time are still needed in the future. Secondly, the current study only focused on the rhesus monkeys naive to antiretroviral therapy. In a recent study, it was proposed that

combination antiretroviral therapy might contribute to the HAND in the era of cART (Gelman 2015). Considering that more and more HIV patients are accessible to antiretroviral therapy but still harassed by HAND, further studies are needed to longitudinally investigate the neurodegeneration of SIV-infected rhesus monkeys under antiretroviral therapy.

Conclusion

In the current study, we found that the WM in the inferotemporal regions was impaired by SIV infection and the axonal injuries might be the neuropathological process behind. We investigated the relationship of peripheral blood indices with the MRI results and found that the WM impairments in iTEpd persisted even though the immune dysfunction in SIV infection alleviated temporally. The MRI findings suggested that the FA might be a sensitive image marker to detect the WM impairments in SIV infection. Future studies with larger sample size would be expected to further explore the SIV associated WM abnormalities and provide insight into the WM degeneration occurred in HIV infection.

Acknowledgments This paper is supported by the National Natural Science Foundation of China under Grant No. 81501549, 81371635, 81571649, 81227901, 61231004, 81171314, and 81571634, the National Basic Research Program of China (973 Program) under Grant 2011CB707700, the Key Research Program of the Chinese Academy of Sciences under Grant No. KGZD-EW-T03, the Natural Science Foundation of Beijing under Grant No. 7132108, the Beijing Municipal Administration of Hospitals Clinical Medicine Development of Special Funding Support under Grant No. ZYLX201511, and the capital health research and development of special under Grant No. 2011-2018-01. The authors also would like to express their deep appreciation to all anonymous reviewers for their kind comments.

Conflict of interest The authors declare that they have no conflict of interest. The authors alone are responsible for the content and writing of the paper.

References

- Anthony IC, Bell JE (2008) The neuropathology of HIV/AIDS. *Int Rev Psychiatry* 20:15–24
- Bao R, Zhuang K, Liu J, Wu J, Li J, Wang X, Ho WZ (2014) Lipopolysaccharide induces immune activation and SIV replication in rhesus macaques of Chinese origin. *PLoS One* 9, e98636
- Basser PJ, Mattiello J, LeBihan D (1994) MR diffusion tensor spectroscopy and imaging. *Biophys J* 66:259–267
- Becker JT, Maruca V, Kingsley LA, Sanders JM, Alger JR, Barker PB, Goodkin K, Martin E, Miller EN, Ragin A, Sacktor N, Selnes O, Multicenter ACS (2012) Factors affecting brain structure in men with HIV disease in the post-HAART era. *Neuroradiology* 54: 113–121
- Bell JE (1998) The neuropathology of adult HIV infection. *Rev Neurol (Paris)* 154:816–829

- Burudi EM, Fox HS (2001) Simian immunodeficiency virus model of HIV-induced central nervous system dysfunction. *Adv Virus Res* 56:435–468
- Chen Y, An H, Zhu H, Stone T, Smith JK, Hall C, Bullitt E, Shen D, Lin W (2009) White matter abnormalities revealed by diffusion tensor imaging in non-demented and demented HIV+ patients. *Neuroimage* 47:1154–1162
- Clifford DB, Ances BM (2013) HIV-associated neurocognitive disorder. *Lancet Infect Dis* 13:976–986
- Correa DG, Zimmermann N, Doring TM, Wilner NV, Leite SC, Cabral RF, Fonseca RP, Bahia PR, Gasparetto EL (2015) Diffusion tensor MR imaging of white matter integrity in HIV-positive patients with planning deficit. *Neuroradiology*
- Ellis R, Langford D, Masliah E (2007) HIV and antiretroviral therapy in the brain: neuronal injury and repair. *Nat Rev Neurosci* 8:33–44
- Gelman BB (2015) Neuropathology of HAND with suppressive antiretroviral therapy: encephalitis and neurodegeneration reconsidered. *Curr HIV/AIDS Rep* 12:272–279
- Gold LH, Fox HS, Henriksen SJ, Buchmeier MJ, Weed MR, Taffe MA, Huitron-Resendiz S, Horn TF, Bloom FE (1998) Longitudinal analysis of behavioral, neurophysiological, viral and immunological effects of SIV infection in rhesus monkeys. *J Med Primatol* 27:104–112
- Gongvatana A, Schweinsburg BC, Taylor MJ, Theilmann RJ, Letendre SL, Alhassoon OM, Jacobus J, Woods SP, Jernigan TL, Ellis RJ, Frank LR, Grant I, Charter G (2009) White matter tract injury and cognitive impairment in human immunodeficiency virus-infected individuals. *J Neurovirol* 15:187–195
- Gongvatana A, Cohen RA, Correia S, Devlin KN, Miles J, Kang H, Ombao H, Navia B, Laidlaw DH, Tashima KT (2011) Clinical contributors to cerebral white matter integrity in HIV-infected individuals. *J Neurovirol* 17:477–486
- Gosztonyi G, Artigas J, Lamperth L, Webster HD (1994) Human immunodeficiency-virus (Hiv) distribution in Hiv encephalitis - study of 19 cases with combined Use of in-situ hybridization and immunocytochemistry. *J Neuropathol Exp Neurol* 53:521–534
- Heaton RK, Clifford DB, Franklin DR Jr, Woods SP, Ake C, Vaida F, Ellis RJ, Letendre SL, Marcotte TD, Atkinson JH, Rivera-Mindt M, Vigil OR, Taylor MJ, Collier AC, Marra CM, Gelman BB, McArthur JC, Morgello S, Simpson DM, McCutchan JA, Abramson I, Gamst A, Fennema-Notestine C, Jernigan TL, Wong J, Grant I, Group C (2010) HIV-associated neurocognitive disorders persist in the era of potent antiretroviral therapy: CHARTER study. *Neurology* 75:2087–2096
- Hoare J, Fouche JP, Spottiswoode B, Sorsdahl K, Combrinck M, Stein DJ, Paul RH, Joska JA (2011) White-matter damage in clade C HIV-positive subjects: a diffusion tensor imaging study. *J Neuropsychiatry Clin Neurosci* 23:308–315
- Hoare J, Fouche JP, Spottiswoode B, Donald K, Philipps N, Bezuidenhout H, Mulligan C, Webster V, Oduro C, Schrieff L, Paul R, Zar H, Thomas K, Stein D (2012) A diffusion tensor imaging and neurocognitive study of HIV-positive children who are HAART-naïve “slow progressors”. *J Neurovirol* 18:205–212
- Howell BR, McCormack KM, Grand AP, Sawyer NT, Zhang X, Maestripieri D, Hu X, Sanchez MM (2013) Brain white matter microstructure alterations in adolescent rhesus monkeys exposed to early life stress: associations with high cortisol during infancy. *Biol Mood Anxiety Disord* 3:21
- Howell BR, Godfrey J, Gutman DA, Michopoulos V, Zhang X, Nair G, Hu X, Wilson ME, Sanchez MM (2014) Social subordination stress and serotonin transporter polymorphisms: associations with brain white matter tract integrity and behavior in juvenile female macaques. *Cereb Cortex* 24:3334–3349
- Kravitz DJ, Saleem KS, Baker CI, Mishkin M (2011) A new neural framework for visuospatial processing. *Nat Rev Neurosci* 12:217–230
- Kravitz DJ, Saleem KS, Baker CI, Ungerleider LG, Mishkin M (2013) The ventral visual pathway: an expanded neural framework for the processing of object quality. *Trends Cogn Sci* 17:26–49
- Kuper M, Rabe K, Esser S, Gizewski ER, Husstedt IW, Maschke M, Obermann M (2011) Structural gray and white matter changes in patients with HIV. *J Neurol* 258:1066–1075
- Langford TD, Letendre SL, Marcotte TD, Ellis RJ, McCutchan JA, Grant I, Mallory ME, Hansen LA, Archibald S, Jernigan T, Masliah E, Group H (2002) Severe, demyelinating leukoencephalopathy in AIDS patients on antiretroviral therapy. *AIDS* 16:1019–1029
- Leite SC, Correa DG, Doring TM, Kubo TT, Netto TM, Ferracini R, Ventura N, Bahia PR, Gasparetto EL (2013) Diffusion tensor MRI evaluation of the corona radiata, cingulate gyri, and corpus callosum in HIV patients. *J Magn Reson Imaging* 38:1488–1493
- Lentz MR, Kim WK, Lee V, Bazner S, Halpern EF, Venna N, Williams K, Rosenberg ES, Gonzalez RG (2009) Changes in MRS neuronal markers and T cell phenotypes observed during early HIV infection. *Neurology* 72:1465–1472
- Li C, Zhang X, Komery A, Li Y, Novembre FJ, Herndon JG (2011) Longitudinal diffusion tensor imaging and perfusion MRI investigation in a macaque model of neuro-AIDS: a preliminary study. *Neuroimage* 58:286–292
- Masters MC, Ances BM (2014) Role of neuroimaging in HIV-associated neurocognitive disorders. *Semin Neurol* 34:89–102
- McLaren DG, Kosmatka KJ, Oakes TR, Kroenke CD, Kohama SG, Matochik JA, Ingram DK, Johnson SC (2009) A population-average MRI-based atlas collection of the rhesus macaque. *Neuroimage* 45:52–59
- Medana IM, Esiri MM (2003) Axonal damage: a key predictor of outcome in human CNS diseases. *Brain* 126:515–530
- Murray EA, Rausch DM, Lendvay J, Sharer LR, Eiden LE (1992) Cognitive and motor impairments associated with SIV infection in rhesus monkeys. *Science* 255:1246–1249
- Nir TM, Jahanshad N, Busovaca E, Wendelken L, Nicolas K, Thompson PM, Valcour VG (2014) Mapping white matter integrity in elderly people with HIV. *Hum Brain Mapp* 35:975–992
- Ohyama K, Sugase-Miyamoto Y, Matsumoto N, Sato C, Shidara M (2014) Small effect of upcoming reward outcomes on visual cue-related neuronal activity in macaque area TE during conditional associations. *Neurosci Res* 88:28–38
- Pfefferbaum A, Rosenbloom MJ, Adalsteinsson E, Sullivan EV (2007) Diffusion tensor imaging with quantitative fibre tracking in HIV infection and alcoholism comorbidity: synergistic white matter damage. *Brain* 130:48–64
- Raja F, Sheriff FE, Morris CS, Bridges LR, Esiri MM (1997) Cerebral white matter damage in HIV infection demonstrated using beta-amyloid precursor protein immunoreactivity. *Acta Neuropathol* 93:184–189
- Sainz T, Serrano-Villar S, Diaz L, Gonzalez Tome MI, Gurbindo MD, de Jose MI, Mellado MJ, Ramos JT, Zamora J, Moreno S, Munoz-Fernandez MA (2013) The CD4/CD8 ratio as a marker T-cell activation, senescence and activation/exhaustion in treated HIV-infected children and young adults. *AIDS* 27:1513–1516
- Saleem KS, Logothetis NK (2012) A combined MRI and histology atlas of the rhesus monkey brain in stereotaxic coordinates. Academic Press
- Saracino A, Bruno G, Scudeller L, Volpe A, Caricato P, Ladisa N, Monno L, Angarano G (2014) Chronic inflammation in a long-term cohort of HIV-infected patients according to the normalization of the CD4:CD8 ratio. *AIDS Res Hum Retroviruses* 30:1178–1184
- Sarma MK, Nagarajan R, Keller MA, Kumar R, Nielsen-Saines K, Michalik DE, Deville J, Church JA, Thomas MA (2014) Regional brain gray and white matter changes in perinatally HIV-infected adolescents. *Neuroimage Clin* 4:29–34
- Schouten J, Cinque P, Gisslen M, Reiss P, Portegies P (2011) HIV-1 infection and cognitive impairment in the cART era: a review. *AIDS* 25:561–575

- Serrano-Villar S, Gutierrez C, Vallejo A, Hernandez-Novoa B, Diaz L, Abad Fernandez M, Madrid N, Dronza F, Zamora J, Munoz-Fernandez MA, Moreno S (2013) The CD4/CD8 ratio in HIV-infected subjects is independently associated with T-cell activation despite long-term viral suppression. *J Infect* 66:57–66
- Sewards TV (2011a) Adolf Hopf's 1954 myeloarchitectonic parcellation of the human temporal lobe: a review and assessment. *Brain Res Bull* 86:298–313
- Sewards TV (2011b) Neural structures and mechanisms involved in scene recognition: a review and interpretation. *Neuropsychologia* 49:277–298
- Smith SM (2002) Fast robust automated brain extraction. *Hum Brain Mapp* 17:143–155
- Smith SM, Jenkinson M, Woolrich MW, Beckmann CF, Behrens TE, Johansen-Berg H, Bannister PR, De Luca M, Drobnjak I, Flitney DE, Niazy RK, Saunders J, Vickers J, Zhang Y, De Stefano N, Brady JM, Matthews PM (2004) Advances in functional and structural MR image analysis and implementation as FSL. *Neuroimage* 23(Suppl 1):S208–S219
- Smith SM, Jenkinson M, Johansen-Berg H, Rueckert D, Nichols TE, Mackay CE, Watkins KE, Ciccarelli O, Cader MZ, Matthews PM, Behrens TE (2006) Tract-based spatial statistics: voxelwise analysis of multi-subject diffusion data. *Neuroimage* 31:1487–1505
- Stubbe-Drger B, Deppe M, Mohammadi S, Keller SS, Kugel H, Gregor N, Evers S, Young P, Ringelstein EB, Arendt G, Knecht S, Husstedt IW, German Competence Network HA (2012) Early microstructural white matter changes in patients with HIV: a diffusion tensor imaging study. *BMC Neurol* 12:23
- Sun SW, Liang HF, Trinkaus K, Cross AH, Armstrong RC, Song SK (2006) Noninvasive detection of cuprizone induced axonal damage and demyelination in the mouse corpus callosum. *Magn Reson Med* 55:302–308
- Thornhill J, Inshaw J, Oomeer S, Kaleebu P, Cooper D, Ramjee G, Schechter M, Tambussi G, Fox J, Miro JM, Weber J, Babiker A, Porter K, Fidler S (2014) Enhanced normalisation of CD4/CD8 ratio with early antiretroviral therapy in primary HIV infection. *J Int AIDS Soc* 17:19480
- Williams R, Bokhari S, Silverstein P, Pinson D, Kumar A, Buch S (2008) Nonhuman primate models of NeuroAIDS. *J Neurovirol* 14:292–300
- Winkler AM, Ridgway GR, Webster MA, Smith SM, Nichols TE (2014) Permutation inference for the general linear model. *Neuroimage* 92:381–397
- Woolrich MW, Jbabdi S, Patenaude B, Chappell M, Makni S, Behrens T, Beckmann C, Jenkinson M, Smith SM (2009) Bayesian analysis of neuroimaging data in FSL. *Neuroimage* 45:S173–S186
- Wright PW, Heaps JM, Shimony JS, Thomas JB, Ances BM (2012) The effects of HIV and combination antiretroviral therapy on white matter integrity. *AIDS* 26:1501–1508
- Wu Y, Storey P, Cohen BA, Epstein LG, Edelman RR, Ragin AB (2006) Diffusion alterations in corpus callosum of patients with HIV. *AJNR Am J Neuroradiol* 27:656–660
- Zhu T, Zhong J, Hu R, Tivarus M, Ekholm S, Harezlak J, Ombao H, Navia B, Cohen R, Schifitto G (2013) Patterns of white matter injury in HIV infection after partial immune reconstitution: a DTI tract-based spatial statistics study. *J Neurovirol* 19:10–23